JCS ePress online publication date 23 January 2003

Live-cell monitoring of tyrosine phosphorylation in focal adhesions following microtubule disruption

Jochen Kirchner, Zvi Kam, Gila Tzur, Alexander D. Bershadsky and Benjamin Geiger*

Department of Molecular Cell Biology, The Weizmann Institute of Science, 76100 Rehovot, Israel

*Author for correspondence (e-mail: benny.geiger@weizmann.ac.il)

Accepted 19 November 2002
Journal of Cell Science 116, 975-986 © 2003 The Company of Biologists Ltd
doi:10.1242/jcs.00284

Summary

Tyrosine phosphorylation of focal adhesion components is involved in the regulation of focal adhesion formation and turnover, yet the underlying molecular mechanisms are still poorly defined. In the present study, we have used quantitative fluorescence microscopy to investigate the dynamic relationships between the incorporation of new components into growing focal adhesions and tyrosine phosphorylation of these sites. For this purpose, a new approach for monitoring phosphotyrosine levels in live cells was developed, based on a 'phosphotyrosine reporter' consisting of yellow fluorescent protein fused to two consecutive phosphotyrosine-binding Src-homology 2 (SH2)-domains derived from pp60$^{c\text{-}Src}$. This YFP-dSH2 localized to cell-matrix adhesions and its intensity was linearly correlated with that of an anti-phosphotyrosine antibody labeling. The differential increase in vinculin and phosphotyrosine levels was examined in live cells by two-color time-lapse movies of CFP-vinculin and YFP-dSH2. In this study, focal adhesion growth was triggered by microtubule disruption, which was previously shown to stimulate focal adhesion development by inducing cellular contraction. We show here that, 2 minutes after addition of the microtubule-disrupting drug nocodazole, the local densities of the focal adhesion-associated proteins vinculin, paxillin and focal adhesion kinase (FAK) are significantly elevated and the focal adhesion area is increased, whereas elevation in tyrosine phosphorylation inside the growing adhesions occurs only a few minutes later. Phosphotyrosine and FAK density reach their maximum levels after 10 minutes of treatment, whereas vinculin and paxillin levels as well as focal adhesion size continue to grow, reaching a plateau at about 30 minutes. Our findings suggest that protein recruitment and growth of focal adhesions are an immediate and direct result of increased contractility induced by microtubule disruption, whereas tyrosine phosphorylation is activated later.

Movies available online

Key words: Cell-matrix adhesion, Focal adhesions, Tyrosine phosphorylation, Vinculin, Paxillin, Focal adhesion kinase, FAK

Introduction

Integrin-mediated cell-matrix adhesion occurs at specialized sites where integrins directly bind extracellular matrix molecules and couple them to the actin cytoskeleton (for reviews, see Geiger et al., 2001; Zamir and Geiger, 2001). This linkage is mediated by a sub-membrane interconnecting plaque that consists of structural proteins like vinculin, paxillin, talin, α-actinin and tensin, and signaling molecules including tyrosine kinases such as focal adhesion kinase (FAK), serine/threonine kinases and various adapter proteins. The extraordinary molecular complexity of cell-matrix adhesions enables them to fulfil their dual role as modulators of both mechanical cell anchorage and transmembrane signaling (Geiger and Bershadsky, 2001; Sastry and Burridge, 2000). The most common forms of integrin-mediated cell-matrix adhesions in cultured cells are focal adhesions (FAs), fibrillar adhesions and focal complexes. FAs are oval structures, usually a few μm^2 in area, and are associated with the termini of actin stress fibers. Fibrillar adhesions, which are derived from FAs, are elongated contact sites, associated with fibronectin fibrils (Zamir et al., 2001; Pankov et al., 2000). Focal complexes are small, dot-like adhesions that are mainly found at the cell edge and apparently nucleate FA formation (reviewed by Geiger et al., 2001).

The assembly and maintenance of cell-matrix adhesions is regulated by signaling via small GTPases of the Rho family (Clark et al., 1998; Rottner et al., 1999). It was shown that the activation of Rac-1 induces focal complex formation (Nobes and Hall, 1995; Rottner et al., 1999), whereas the introduction of constitutively active Rho-A leads to the formation of large FAs and stress fibers (Ridley et al., 1992). Rho acts by activating several immediate targets, including Rho-associated kinase (ROCK) and mDia that synergistically affect cell-matrix adhesions and the associated microfilament network (Watanabe et al., 1999; Takaishi et al., 2000; Tominaga et al., 2000; Riveline et al., 2001). Active ROCK inhibits myosin light chain phosphatase (Kimura et al., 1996), thus causing the stimulation of actomyosin contractility. In turn, application of local forces by actomyosin contractility stimulates FA and stress fiber formation (Chrzanowska-Wodnicka and Burridge, 1996; Leopoldt et al., 2001), whereas inhibitors of actomyosin contractility induce disruption of these structures (Volberg et al., 1994; Helfman et al., 1999; Zamir et al., 1999; Balaban et al., 2001). Growth of FAs and focal complexes can also be

induced by the application of external local force (Riveline et al., 2001; Kaverina et al., 2002).

Another key regulatory mechanism affecting FA formation and stability is tyrosine phosphorylation. FAK (Calalb et al., 1995) and members of the pp60^{Src} family (Brown and Cooper, 1996) are involved in the phosphorylation of several FA proteins, including paxillin (Turner, 2000), p130^{Cas} (Vuori and Ruoslahti, 1995), tensin (Bockholt and Burridge, 1993) and FAK itself (Schaller, 2001). This phosphorylation provides docking sites for additional molecules that contain phosphotyrosine (PY)-binding domains such as Src-homology 2 (SH2) (for reviews, see Zamir and Geiger, 2001; Pawson et al., 2001). Serum starvation, as well as treatment with actomyosin relaxants or tyrosine kinase inhibitors, reduce PY levels and block the development of FAs (Ridley and Hall, 1994; Chrzanowska-Wodnicka and Burridge, 1994; Barry and Critchley, 1994; Bershadsky et al., 1996). Furthermore, strong activity of PY phosphatases can disrupt FAs (Schneider et al., 1998), whereas their inhibition can stimulate FA assembly, at least transiently (Retta et al., 1996; Ayalon and Geiger, 1997). Interestingly, overexpression of deregulated pp60$^{v\text{-}Src}$ results in high levels of tyrosine phosphorylation and disrupts FAs (Kellie et al., 1986), and Src (–/–) cells form FAs that fail to turn over into fibrillar adhesions (Volberg et al., 2001). Taken together, these data suggest that tyrosine phosphorylation is involved in the formation and turnover of matrix adhesions.

FA growth can also be triggered by microtubule depolymerization in a Rho- and tyrosine phosphorylation-dependent manner (Bershadsky et al., 1996; Enomoto et al., 1996; Zhang et al., 1997; Liu et al., 1998; Pletjushkina et al., 1998). Although the exact mechanism is still unclear, microtubule disruption appears to promote FA growth by increasing overall actomyosin contractility (Bershadsky et al., 1996). Interestingly, microtubules also seem to influence the formation and turnover of cell-matrix adhesions locally (Kaverina et al., 1999) and the effect of microtubule disruption on FAs and cell motility can be abolished by local application of contractility inhibitors (Kaverina et al., 2000). Together, these results suggest that microtubules suppress FA growth by local inhibition of actomyosin contractility. Nocodazole-mediated stimulation of FA growth might therefore mimic a natural release of FA from this negative regulation.

In this study, we investigated the involvement of tyrosine phosphorylation in nocodazole-induced FA assembly. In addition to analysis of fixed specimens using quantitative immunofluorescence microscopy, we introduced a new technique that made it possible to monitor PY dynamics in live cells. For this purpose, we employed a YFP derivative of the PY-binding SH2 domain of pp60$^{c\text{-}Src}$ (YFP-dSH2). Using this approach, we demonstrated that the increase in tyrosine phosphorylation occurs only after an apparent recruitment of several FA proteins takes place and does not directly correlate with FA growth. Thus, microtubule-disruption-induced tension stimulates the binding of new molecules such as vinculin, paxillin and FAK to FAs independently of a local increase in tyrosine phosphorylation.

Materials and Methods

Cell culture and immunofluorescence staining

SV80 cells were cultured in Dulbecco's modified Eagle's medium (DMEM) supplemented with 10% bovine calf serum. For immunofluorescence labeling, cells were seeded on glass coverslips. For transfection, cells were plated at 20-25% confluence and calcium phosphate transfection was carried out 24 hours later as previously described (Sambrook et al., 1989). To explore the changes in FAs induced by microtubule disruption, cells were serum starved for 24 hours and then treated with DMEM containing 10 μM nocodazole (Sigma) for up to 60 minutes. For immunofluorescence labeling, cells were permeabilized and fixed with 3% paraformaldehyde + 0.5% Triton X-100 in PBS for 2 minutes and then further fixed for 45 minutes in 3% paraformaldehyde in PBS. Fixed cells were washed twice for 10 minutes in PBS and stained with the primary antibody for 1 hour. After washing in PBS for 3×10 minutes, the cells were labeled with the secondary antibody for 40 minutes, washed in PBS and mounted in Elvanol (Moviol 4-88, Hoechst, Frankfurt, Germany).

Immunochemical reagents

The rabbit anti-PY antiserum was kindly provided by Israel Pecht and Arie Licht (The Weizmann Institute, Rehovot). Anti-vinculin (α-Hvin) monoclonal antibody was from Sigma. Anti-FAK and anti-paxillin monoclonal antibodies were from Transduction Laboratories (Lexington, KY). All secondary antibodies were from Jackson ImmunoResearch Laboratories (West Grove, PA).

Generation of YFP-SH2 constructs

The pp60Src SH2 domain (corresponding to amino acids 142-251) (Martinez et al., 1987) was amplified by PCR, adding 5′ *Hin*dIII and 3′ *Xba*I sites to the sequence. This DNA was then inserted in-frame into the corresponding sites in the EYFP-C3 vector modified from EGFP-C3 vector (Clontech, Palo Alto, CA). To generate the YFP-dSH2 construct, the SH2 domain was amplified again, but this time with a *Hin*dIII site attached to both ends of the fragment. This piece of DNA was then ligated to the *Hin*dIII site of YFP-SH2, and clones containing the insert in the correct orientation were selected. To create the mutated SH2 domain, a primer containing the desired changes (R183A) was used to generate the part of the SH2 upstream of the mutation. The resulting PCR fragment was then used as a 5′ primer in a second PCR as previously described (Landt et al., 1990). The PCR fragment of the mutated SH2 domain was then cloned into EYFP-C3 analogous to the wild-type construct to generate mutated YFP-SH2.

Digital microscopy

Immunofluorescence microscopy of fixed samples was carried out with a Zeiss Axiovert 100 microscope equipped with a ×100/1.4 NA plan-Neofluar objective (Zeiss, Oberkochen, Germany). Images were acquired with a DeltaVision system (Applied Precision Inc., Issaqua, WA) as previously described (Zamir et al., 1999), except that the pixel size was 0.066 μm. Image acquisition and processing were performed with Resolve3D and Priism programs as described (Zamir et al., 1999).

For dynamic studies, cells were cultured in coverslip-bottom dishes (MatTek corporation, Ashland, MA). 12 hours after transfection, the cells were serum starved for another 12 hours. The carbonate-buffered DMEM was then exchanged for DMEM containing 25 mM HEPES (Bio Lab, Jerusalem, Israel) and nocodazole was added 30 minutes thereafter. Live-cell imaging was carried out with a back-illuminated frame transfer grade 1 Quantics CCD camera equipped with an EEV 57-10 G1 Chip (Photometrics, Tucson, AZ), generating 12-bit digital data. The microscope contained a filter set for Cyan GFP (No. F31-044, AHF Analysentechnik, Tübingen, Germany) and a nonselective FITC filter set (Zeiss, Oberkochen, Germany), which was used to record YFP. The objective and stage were heated to maintain the cells at a stable temperature of 37°C throughout the experiment. Images

were taken every minute for 30 minutes after addition of nocodazole and processed in the same way as in the case of fixed samples. For the measurements of YFP-dSH2 fluorescence, we first determined the range of fluorescence intensity, which corresponds to YFP-dSH2 expression level exerting no apparent effects on PY staining and appearance of FAs. All further measurements were conducted on cells expressing YFP-dSH2 in that range.

Results

Nocodazole treatment differentially stimulates FA assembly and local tyrosine phosphorylation

Serum starvation of SV80 cells induces a dramatic deterioration of FAs and accumulation of small (less than 1 μm in diameter) PY-containing focal complexes. Vinculin was hardly detectable in these structures, except for a narrow zone along their margins, closer to the cell center (Fig. 1, control). Paxillin and FAK labeling of these focal complexes was more prominent, exhibiting varying degrees of overlap with PY (see ratio images, Figs 2, 3). After 3 minutes of treatment with 10 μM nocodazole, an increase in the labeling intensity and size of the vinculin-, paxillin- and FAK-containing adhesions was noted (Fig. 4). For vinculin and paxillin, the growth of the initial adhesions was highly polar, progressing towards the cell center. This is clearly evident from the ratio images in Figs 1 and 2 (in the 3-minute panels), where the protein labeling (red-labeled rim) is uniformly oriented towards the cell center. By contrast, FAK was more broadly distributed over the entire area of the developing adhesion (Fig. 3, ratio image, 3 minutes). Interestingly, the labeling intensity for PY and the size of the PY-rich dots hardly increased following 3 minutes of nocodazole treatment.

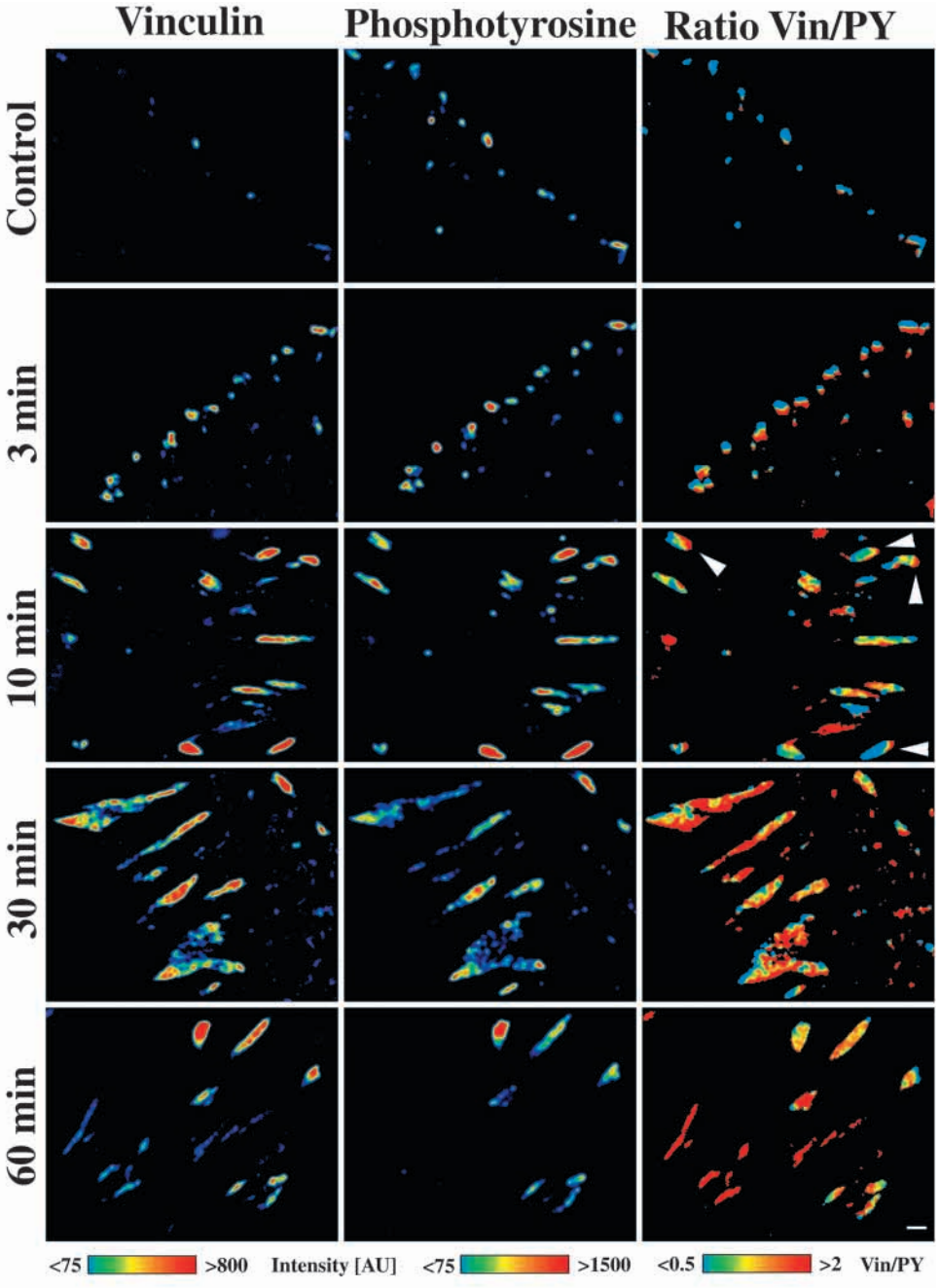

Fig. 1. Double immunostaining of serum-starved SV80 cells for vinculin (left column) and phosphotyrosine (middle column) following treatment with nocodazole for up to 60 minutes. The right column shows the ratio between vinculin and PY intensities. All images are presented in a spectrum scale as indicated in the lookup table for each column. Although focal complexes are most prominent at time=0, FAs are apparent at 3 minutes, and constitute the majority of adhesive structures from 10 minutes onwards. FAs reach their maximal size at 30 minutes. Vinculin intensity increases from 0 to 30 minutes. Note the 'centripetal shift' of vinculin relative to PY at 0 and 3 minutes, which can still be seen in some FAs after 10 minutes (arrowheads). Bar, 1 μm.

By 10 minutes of incubation with nocodazole, the adhesion sites became elongated, reaching several μm in length. The labeling intensity for all three tested proteins and of PY also increased (Fig. 4). The internal distribution of PY and the three proteins within the newly formed FA was often non-uniform; commonly, vinculin was enriched at the pole of FAs, pointing to the cell center (Fig. 1, arrowheads). A similar shift was also occasionally observed with paxillin. Upon longer incubation (up to 30 minutes), the local intensities of vinculin and paxillin, as well as the size of FAs, continued to increase, and then declined. By contrast, FAK and PY intensity reached a plateau at 10 minutes and sharply declined at 1 hour after addition of the drug. Taken

together, these data indicate that the tension-induced binding of FA components and FA growth precede the stimulation of local tyrosine phosphorylation, and that different FA components may display different recruitment kinetics.

The dynamics of tyrosine phosphorylation following nocodazole treatment: use of YFP-dSH2 as a PY reporter in live cells

In view of the rapid local changes in tyrosine phosphorylation observed upon nocodazole stimulation, it was desirable to examine, in real-time, the dynamic changes of PY levels in FAs of live cells. Towards this end, we constructed novel, intrinsically fluorescent, 'PY reporters', namely YFP-fusion proteins containing one or two copies of the PY-binding domain (SH2) of $pp60^{Src}$ (Fig. 5A,B). Both molecules localized in cultured cells to FAs, although theYFP-SH2 fusion protein (C) produced a higher cytoplasmic background than YFP-dSH2 (D). By contrast, a SH2 domain mutated at Argβb5 (R183A), which has a 200-fold reduced affinity to PY (Bradshaw et al., 1999), did not show any FA localization at all. The FA localization of YFP-SH2 was not retained after fixation and permeabilization of the cells (E), whereas FA-associated YFP-dSH2 was also found in FA of fixed cells (F). We therefore used the YFP-dSH2 construct for live-cell experiments.

In order to test whether YFP-dSH2 can be used as a reliable quantitative reporter for local PY levels, we transfected SV80 cells with YFP-dSH2, fixed the cells 24 hours later and stained them with an anti-PY antibody. The images showing the YFP-dSH2 distribution (Fig. 6A,B) and the corresponding anti-PY staining (C,D) were then subjected to ratio imaging and quantitative analysis. The images in Fig. 6 (E,F) represent, in the spectrum scale, the ratio between the intensities of YFP fluorescence and the fluorescence of the fluorochrome (Cy3) conjugated with the secondary antibody used for visualizing PY. This ratio was highly uniform inside the same cell, and throughout individual FAs (E,F).

The relationship between the PY antibody and YFP-dSH2 labeling was studied further by plotting, against each other, the intensities of the two labels measured for individual FAs. As can be seen in Fig. 6 (G,H), the two labels show a linear correlation over a wide range of expression levels. These experiments indicated that expression of particularly high levels of YFP-dSH2 leads to a marked elevation (up to fivefold, compared with nontransfected

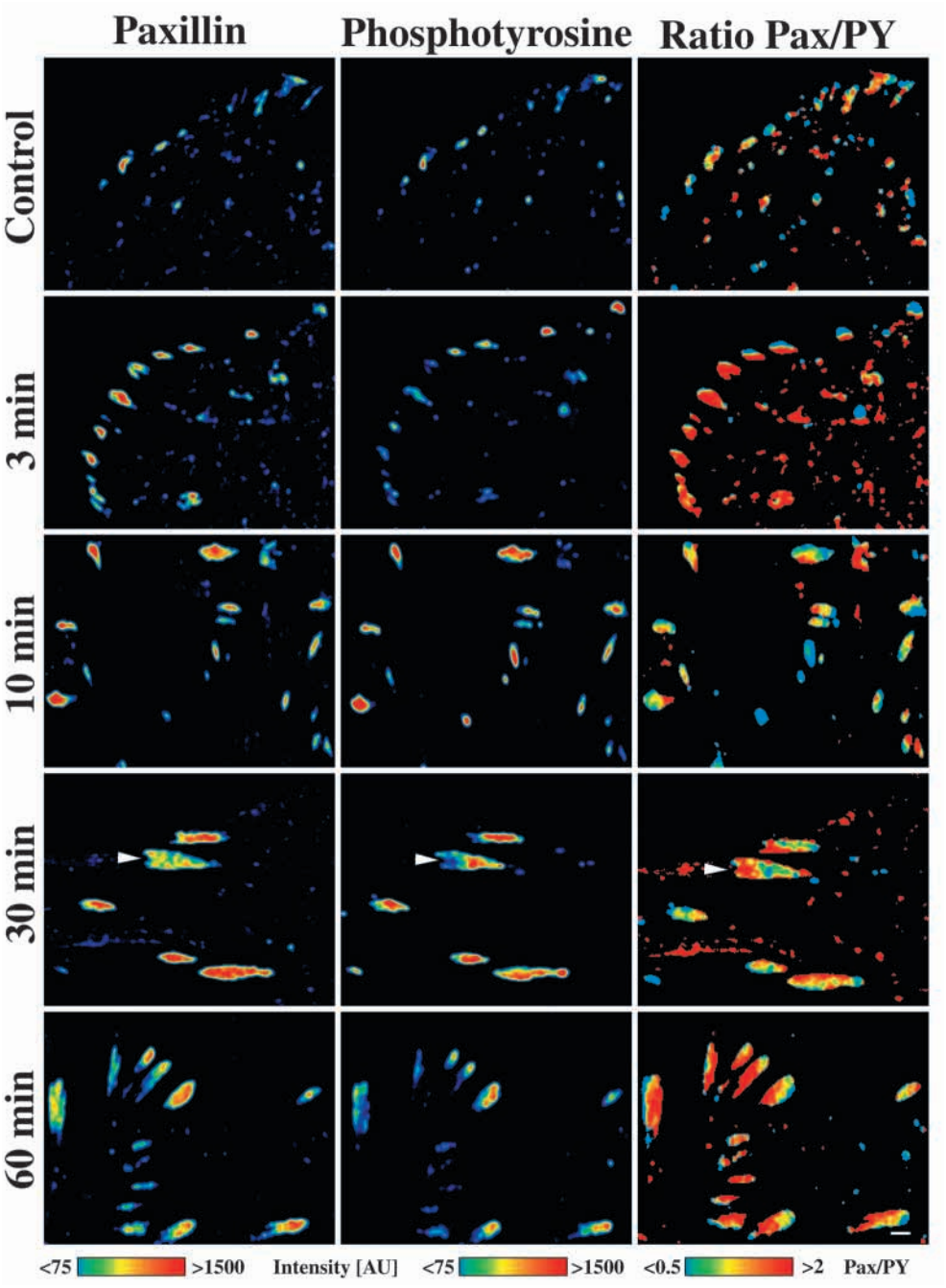

Fig. 2. Double immunostaining of paxillin and phosphotyrosine. All images were acquired and produced as in Fig. 1. Whereas paxillin levels are continuously increasing from 0 to 30 minutes, PY levels increase significantly only later, between 3 and 10 minutes, and then reach a plateau. Note the overall extensive overlap between paxillin and PY labeling. Main differences are detected along the paxillin-rich and PY-poor peripheral margins of FAs at 30 minutes (arrowheads). Bar, 1 μm.

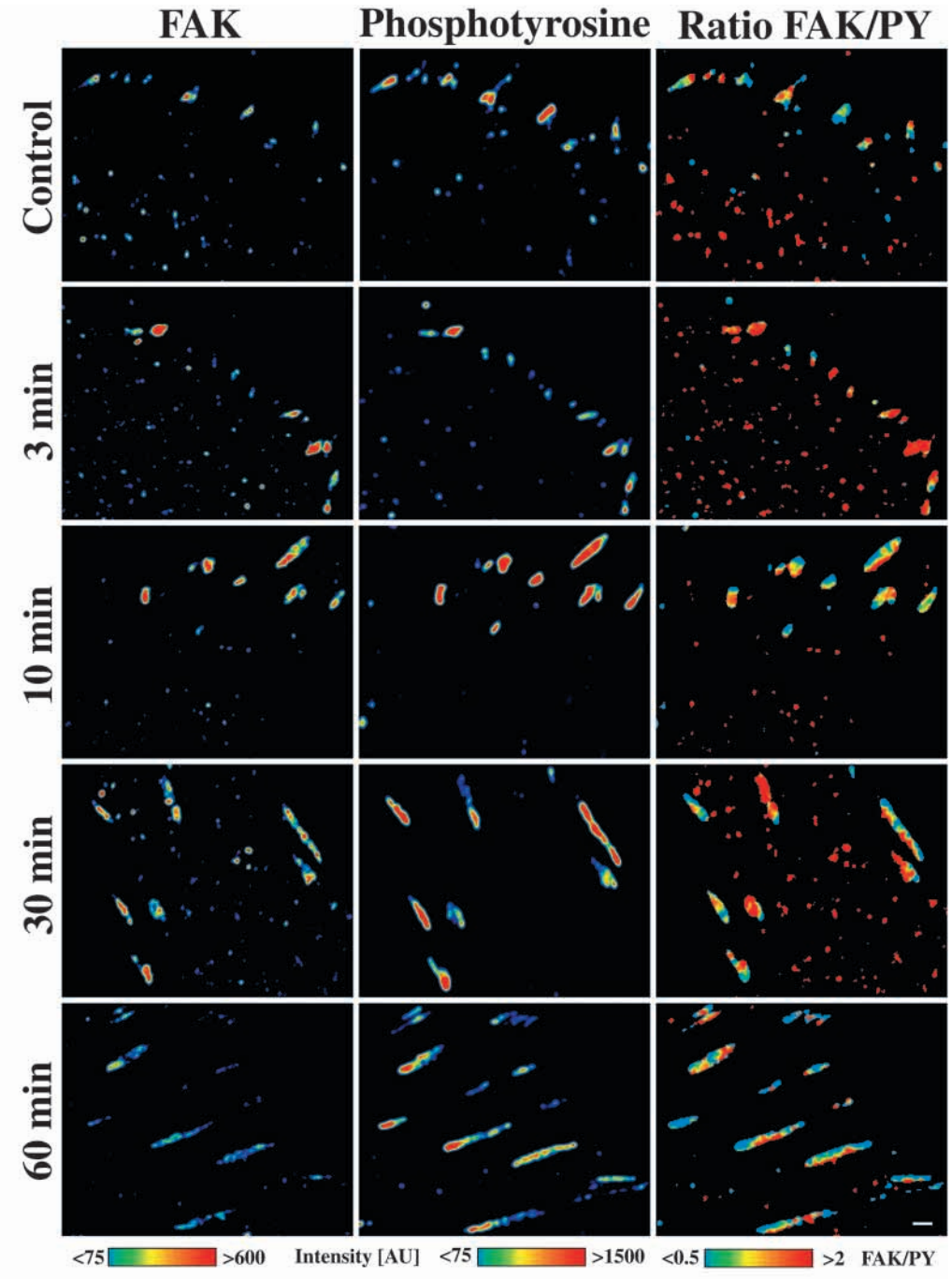

Fig. 3. Double immunostaining of FAK and phosphotyrosine. All images were acquired and processed as in Fig. 1. Note that FAK levels in small adhesions have already increased at 3 minutes, whereas PY levels remain almost unchanged. Both FAK and PY reach their maximal levels at 10 minutes, remain high for up to 30 minutes, and return to control levels by 60 minutes. Bar, 1 μm.

cells) in PY levels (G,H), as well as to a moderate increase in the average size of FAs (quantitative data not shown). By contrast, moderate levels of expression of YFP-dSH2 (see, for example, cell 5 in Fig. 6) have no detectable effect on the intensity of PY labeling as compared with nontransfected cells. Moreover, the high correlation between YFP-dSH2 and anti-PY labeling indicated that the recruitment of the former into phosphorylated adhesion sites is very rapid. Apart from its effect on endogenous PY, we tested the influence of YFP-dSH2 expression on the levels of vinculin, paxillin, FAK and tensin in FAs. These studies indicated that expression of YFP-dSH2 at levels that do not disturb the PY distribution has no effect on the level and organization of these proteins either (data not shown). On the basis of these data, we have regarded YFP-dSH2, when expressed at appropriate levels (e.g. cell 5, but not cells 1 or 4, in Fig. 6), as an essentially nonperturbing quantitative PY reporter. YFP-dSH2 localization to FAs was also observed in several other cell lines, including fibroblasts REF 52, NIH 3T3 and MEF, as well as HeLa and MDCK epithelial cells where cell-cell junctions were also labeled (data not shown).

In order to compare the recruitment of vinculin and the increase in tyrosine phosphorylation in the same cells in real-time, SV80 cells were co-transfected with CFP-vinculin and YFP-dSH2, then serum starved for 12 hours and subjected to nocodazole treatment (see Movie 1, http://jcs.biologists.org/supplemental). Before nocodazole treatment, the residual adhesion sites in the starved cells contain very little vinculin (Fig. 7). Within 2 minutes after application of nocodazole, vinculin starts to accumulate at the cell margins, inside and around peripheral focal complexes and small FAs. After 6 minutes, vinculin becomes confined to FAs, which continue to grow until 10 minutes. By contrast, the early changes in PY levels are much less dramatic and uniform. After 2 minutes, the majority of FAs maintain their initial level of tyrosine phosphorylation, and sometimes show a decrease in tyrosine phosphorylation or even vanish (Fig. 7), whereas a few show a mild increase in PY. By 6 minutes, most adhesions show an increase in YFP-dSH2 levels, which continues until 10 minutes. FA growth according to both labels is almost exclusively oriented towards the cell center. As was already observed with fixed cells (Fig. 1), vinculin is shifted towards the cell center relative to PY.

We also compared, in a quantitative manner, the intensity of

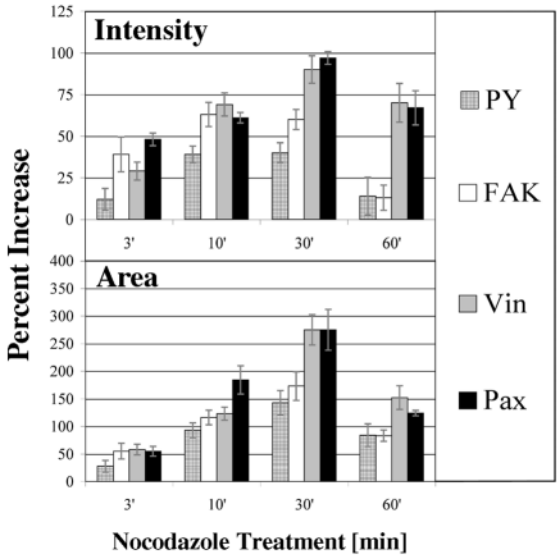

Fig. 4. Quantitative analysis of the immunostaining data shown in Figs 1-3, depicting the percent increase in average intensity and area compared with control, untreated cells. Vinculin, paxillin and FAK levels are already elevated after 3 minutes of treatment, whereas PY levels remain essentially unchanged. Vinculin and paxillin levels continue to increase until 30 minutes and decrease only slightly afterwards, whereas FAK and PY levels reach a plateau after 10 minutes and decrease to control levels between 30 and 60 minutes. FA growth starts immediately and continues for 30 minutes.

CFP-vinculin and YFP-dSH2 in individual adhesions (Fig. 8, I-III). In all three cases shown here, vinculin increases sharply in the first two minutes, whereas the amount of PY present remains almost unchanged. Following a longer incubation, the levels of both vinculin and PY increase. Similar behavior was obtained when the average intensity of all adhesions in the tested cell was calculated.

The two-color movies were very effective for comparing, in real-time, the distribution of different components, but were limited to a relatively small number of double exposures (usually ~10) owing to possible photodamage. To monitor tyrosine phosphorylation dynamics over a longer period and to compare the changes in PY intensity with the growth of FAs, we examined, by time-lapse fluorescence microscopy, cells transfected with YFP-dSH2 alone. The cells were serum starved for 12 hours, treated with nocodazole and examined microscopically for up to 30 minutes. Fig. 9 shows images derived from such a movie (see also Movie 2, http://jcs.biologists.org/supplemental). Each image is the ratio of two different time points (fluorescence ratio of images, 'FRIT image'), highlighting the increase in the area and intensity of PY-positive matrix adhesions induced by nocodazole. The color scale was selected so that structures that remain unchanged between the two time points appear yellow, whereas new structures are depicted in red and those that disappeared are depicted in blue. As shown, some adhesions were formed de novo following addition of nocodazole (Fig. 9, arrow), whereas others disappeared (arrowheads). As was already observed in the vinculin/dSH2 movie, expansion of the tyrosine-phosphorylated area of FA is primarily oriented towards the cell center. Quantitative analysis of FA phosphorylation in selected adhesions (marked on the 6'/2' frame of Fig. 9) shows that all but one of the tested adhesions grow substantially in area (1.5- to 3-fold) during the 30 minutes of stimulation, and the recorded growth and PY dynamics are in good agreement with the data obtained for fixed cells and in the two-color movie. The increase of PY levels in individual adhesions started only 3-5 minutes after nocodazole application and reached maximal values between 6 and 18 minutes after nocodazole stimulation (average time ~10 minutes). It is noteworthy that remarkable differences were observed between the kinetics of tyrosine phosphorylation of individual (sometimes even nearby) FAs within the same cell. For example FA I and III reached

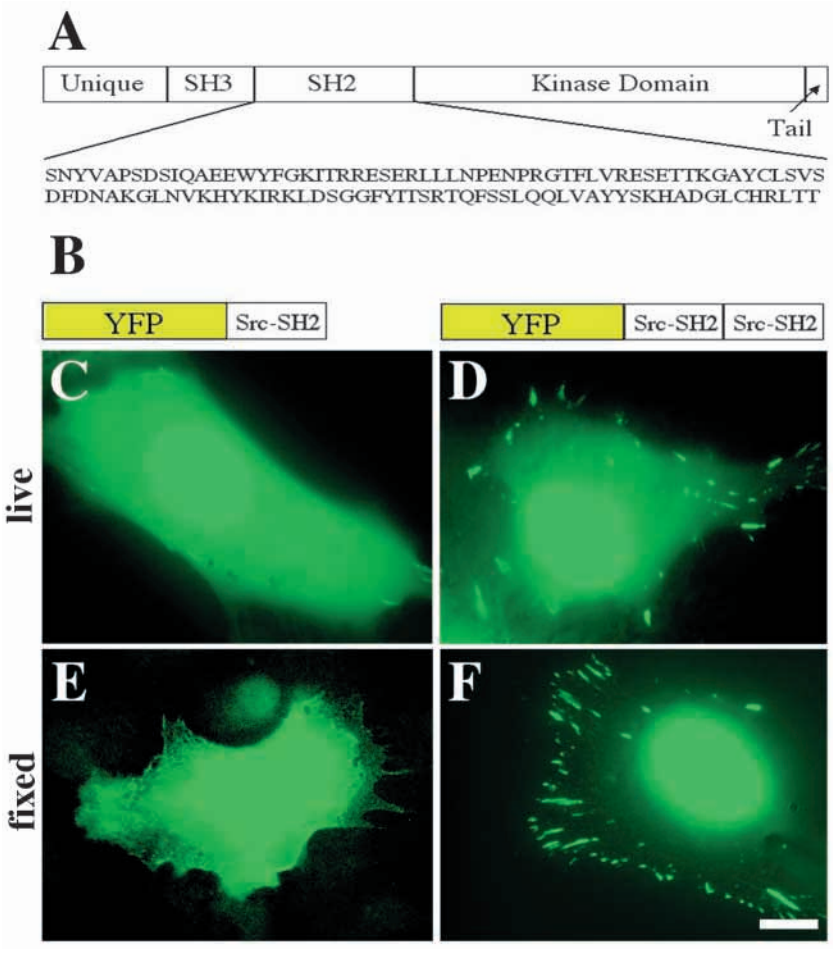

Fig. 5. (A) Domain structure of pp60Src and amino acid sequence of the SH2 domain (from mouse neuronal Src). (B) Schematic representation of the YFP-SH2 and YFP-dSH2 constructs. (C) Live-cell recording of SV80 cells transfected with YFP-SH2. The fusion protein localizes to FAs only weakly and shows a high cytoplasmic background. (D) Live-cell recording of SV80 cells transfected with YFP-dSH2. Note the distinct FA staining and relatively low cytoplasmic background. (E) Fixed cell transfected with YFP-SH2, showing loss of FA localization. (F) Fixed, YFP-dSH2 transfected cell, showing retention of FA labeling after fixation. Bar, 10 μm.

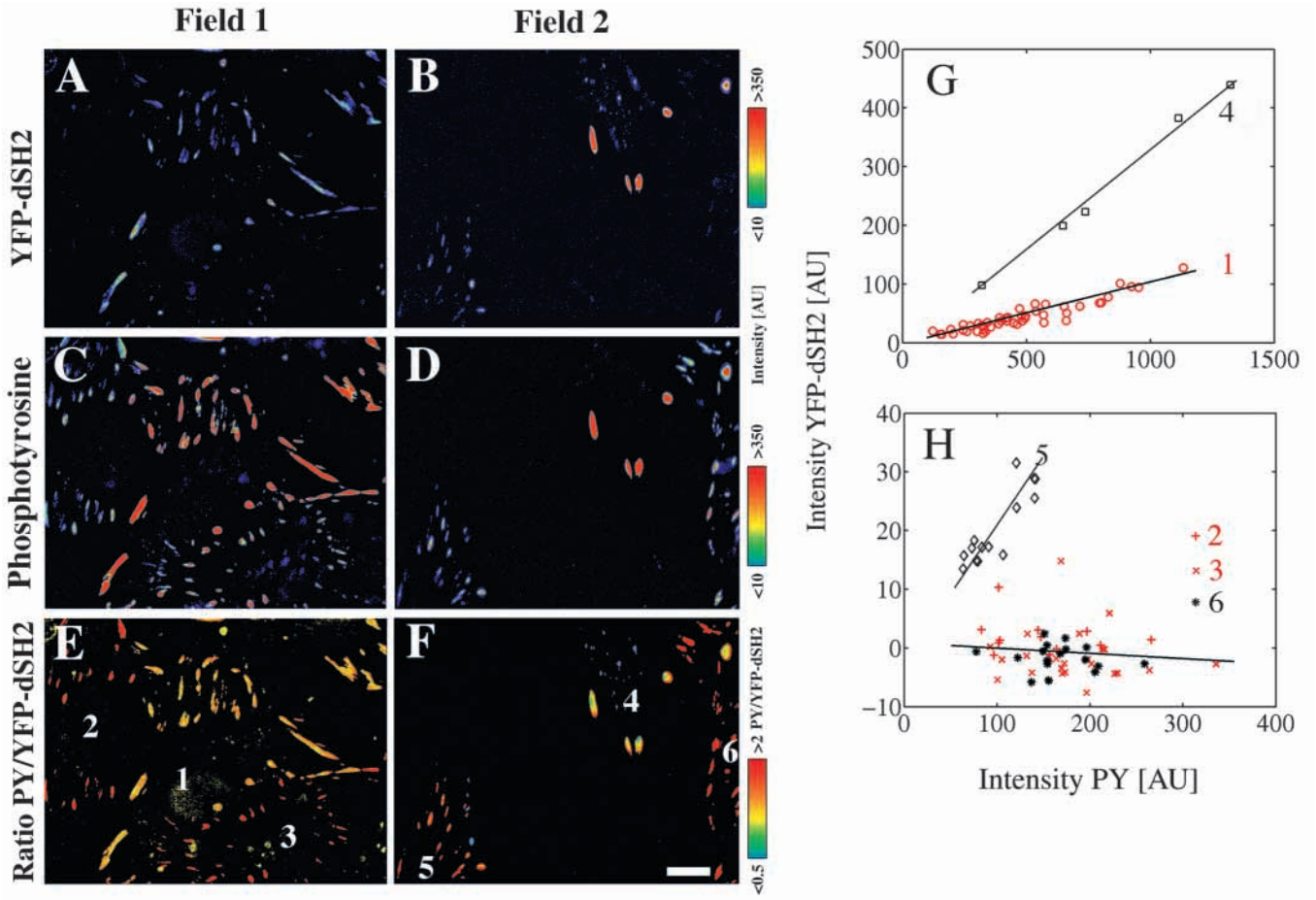

Fig. 6. (A,B) Two fields of YFP fluorescence of SV80 cells transfected with YFP-dSH2. (C,D) Anti-PY staining of the corresponding fields. Images A-D show the fluorescence intensities represented in a spectrum scale, as indicated in the calibration bars. (E,F) Ratio images of the cells shown in (A,C) and (B,D), respectively, depicting the relative fluorescence of PY and YFP-dSH2. The cells shown are numbered consecutively from 1-6. Note the uniform ratio between the two labels in YFP-dSH2 expressing cells (1, 4 and 5), indicating strong correlation between YFP-dSH2 and PY. The cells (2, 3 and 6) showing red FAs (i.e. excess PY) are not expressing detectable levels of YFP-dSH2. (G) Plot of intensity of PY staining against the intensity of labeling in YFP-dSH2-overexpressing cells 1 and 4. (H) Similar plot, as in G, for non-expressing cells 2, 3, 6, and YFP-dSH2 expressing cell 5. FAs from field 1 are represented in red, whereas FAs from field 2 are represented in black. Notice the linear correlation between the two labels, the increase in PY labeling upon expression of particularly high levels of YFP-dSH2, and the normal PY levels in the moderately transfected cell. Bar, 10 μm.

maximal intensity of YFP-dSH2 at 6 minutes (Fig. 9), whereas FA II and IV reached maximal intensity at 18 minutes. Moreover, the extent of local increase in YFP-dSH2 intensity did not correlate with the rate of growth of the adhesion site. For example, the dynamics of local tyrosine phosphorylation were similar for FA I and III (peak at 6 minutes and then decline), yet FA I grew during the whole period, whereas FA III hardly changed.

Discussion

Tyrosine phosphorylation is implicated in the formation, maintenance and turnover of cell-matrix adhesions (Barry and Critchley, 1994; Ridley and Hall, 1994; Chrzanowska-Wodnicka and Burridge, 1994; Bershadsky et al., 1996; Retta et al., 1996; Ayalon and Geiger, 1997; Schneider et al., 1998), yet the mechanism underlying this involvement is still obscure. In this study, we addressed this issue by comparing local changes in PY levels to the recruitment of several FA proteins induced by the microtubule-disrupting drug nocodazole. For this purpose, we have combined quantitative immunofluorescence microscopy with a novel approach for monitoring kinetics of tyrosine phosphorylation in live cells.

FA assembly is a multistage process that involves the transformation of small, dot-like focal complexes into large FAs (see Geiger et al., 2001). Previous studies have shown that application of mechanical force to focal complexes, either by increasing cytoskeletal contractility or by external perturbation, stimulates this transformation (Chrzanowska-Wodnicka and Burridge, 1996; Bershadsky et al., 1996; Leopoldt and Rozengurt, 2001; Riveline et al., 2001) and that this process is centrally coordinated by Rho-family GTPases (Ridley and Hall, 1992; Rottner et al., 1999). It was further proposed that matrix adhesions contain a putative ‘mechanosensor’ whose activation by local tension leads to a cascade of molecular events, including the recruitment of FA proteins, growth of adhesion sites and stimulation of integrin-mediated signaling (reviewed by Geiger and Bershadsky, 2001;

Geiger and Bershadsky, 2002; Riveline et al., 2001). Determining how these three processes are interrelated and elucidating the role of tyrosine phosphorylation were the main objectives of the present work.

We have considered here two alternative mechanisms for force-induced assembly of FAs. One possibility is that mechanical perturbation directly activates local tyrosine phosphorylation which, in turn, creates new docking sites that bind SH2-containing proteins, leading to the recruitment of different plaque proteins and, consequently, to FA consolidation and growth. Alternatively, the activation of the mechanosensor could directly stimulate the binding of new FA proteins, independently of PY signaling.

The present study supports the latter view. We show here that nocodazole-induced changes in FA composition and size are not synchronous. Thus, FA growth is apparent essentially immediately after stimulation, and is accompanied by an increase in the local densities of its constituents, vinculin, paxillin and FAK. By contrast, PY levels are

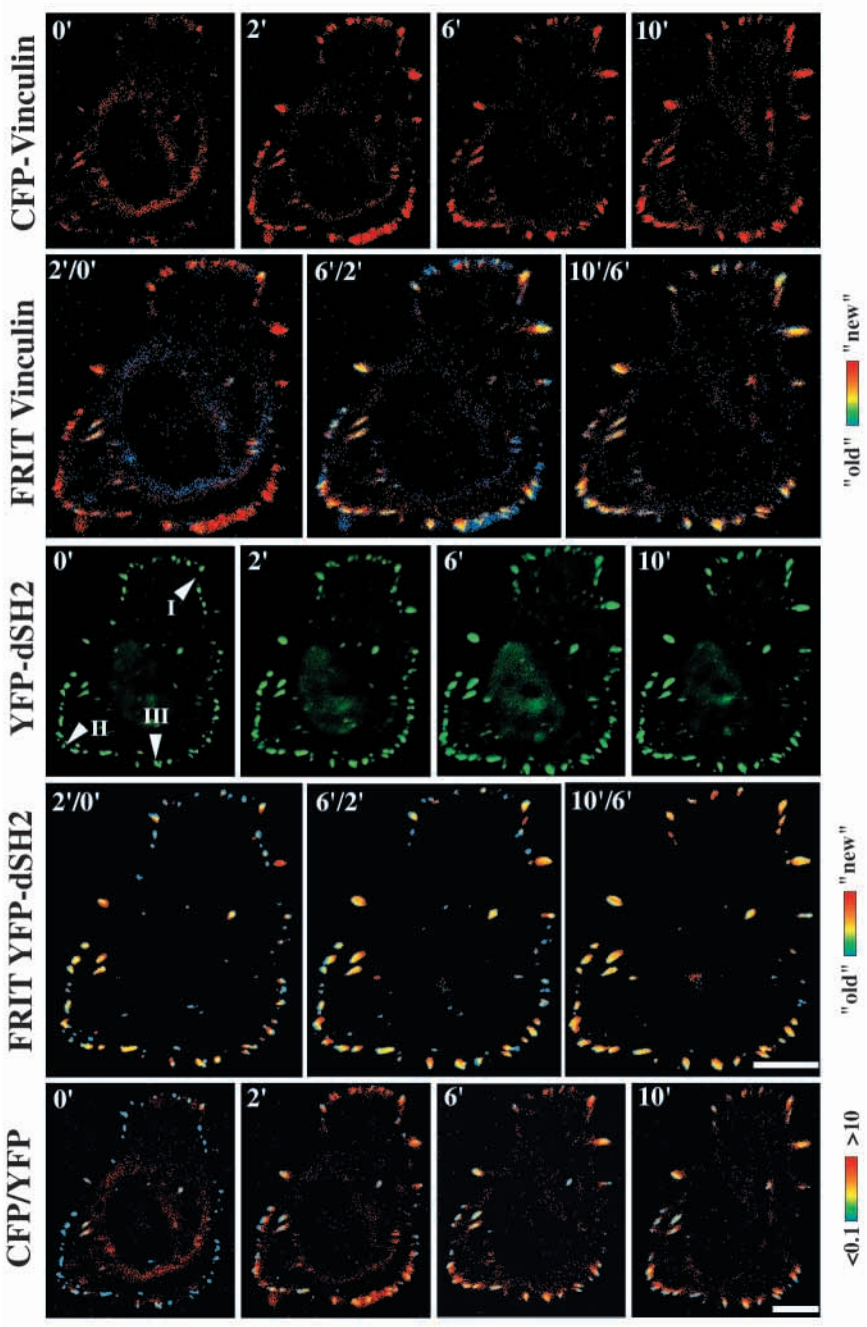

Fig. 7. Frames from a two-color movie showing a serum-starved SV80-cell transfected with CFP-vinculin and YFP-dSH2 and treated with nocodazole. Row 1 shows the CFP-vinculin staining at 4 different time points, and the images in row 2 are time ratio (FRIT) images comparing consecutive time points. Row 3 and 4 show the corresponding YFP-dSH2 images. Row 5 shows the vin/dSH2 ratio at all time points. Note the strong initial increase in vinculin after 2 minutes, in comparison with the low and inconsistent changes in PY levels. The adhesions used for the quantification presented in Fig. 8 are marked in the 0' frame of YFP-dSH2. The whole movie (2 colors and ratio) can be found in the online supplemental material (http://jcs.biologists.org/supplemental). Bar, 10 μm.

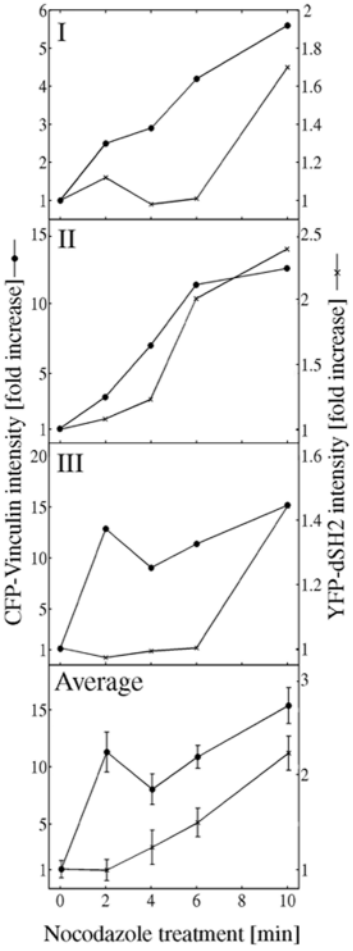

Fig. 8. Quantitative analysis of the three FAs marked in Fig. 7. The temporal changes of the integrated intensities (total label present in each adhesion) of CFP-vinculin and YFP-dSH2 are presented. Note that vinculin intensity increases sharply during the first two minutes in all three cases, whereas there is almost no increase in PY at the same time. The fourth panel shows the average values of all FA-associated CFP-vinculin and YFP-dSH2 in the tested cell, which is consistent with the data obtained for the fixed cells (see Fig. 4).

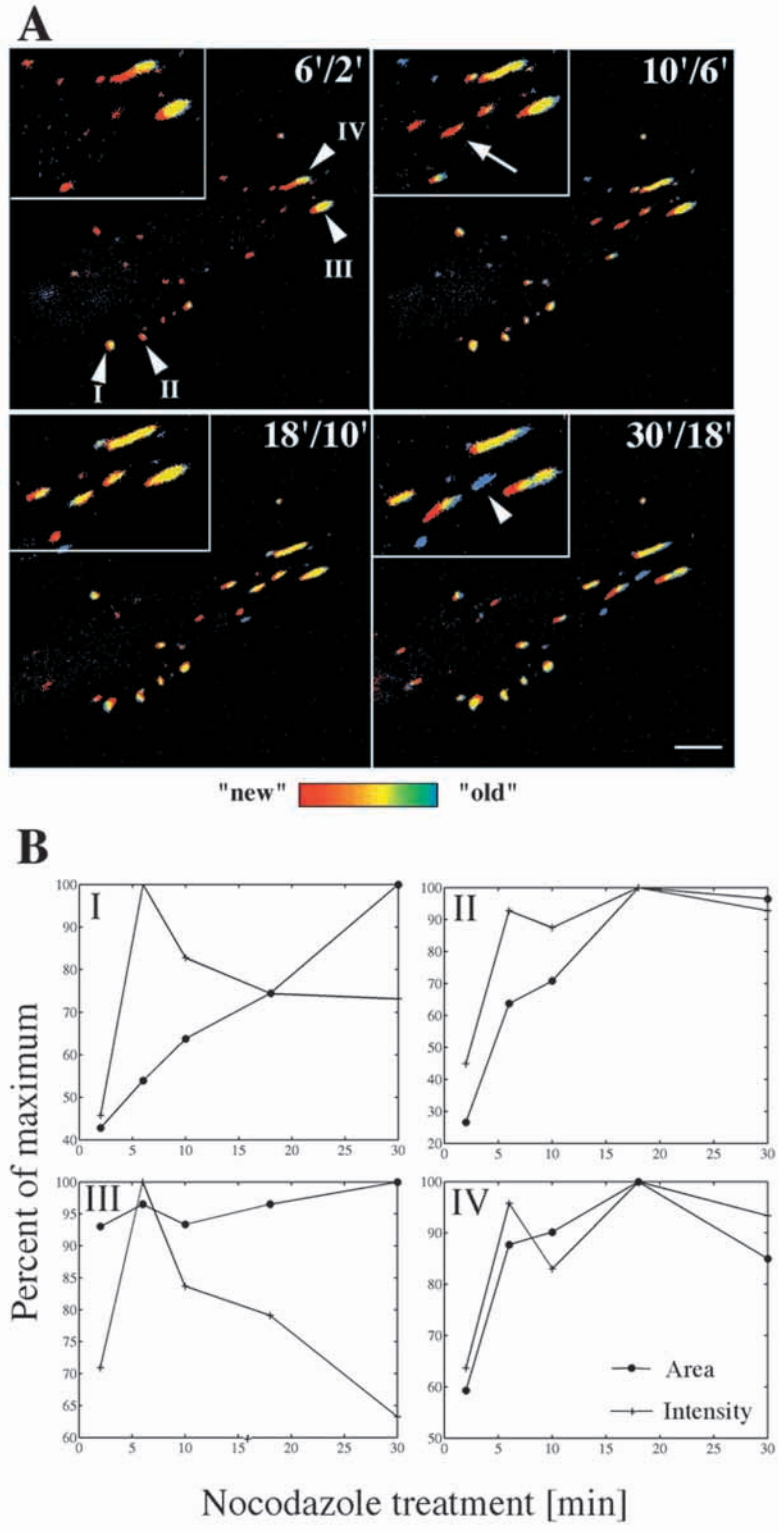

Fig. 9. (A) FRIT images (fluorescence ratio of images taken at different time points) of a movie showing an SV80 cell transfected with YFP-dSH2, serum starved, and treated with nocodazole for 30 minutes. The four spectrum scale images (see lookup table) are temporal ratios of two consecutive frames. Structures that appear only at the later image are shown in red, whereas structures that appear only at the earlier of the two time points are blue. Unchanged structures are represented in yellow. The numbers inserted into the 6'/2' image mark FAs that were further subjected to quantitative analysis (see below). The arrow points to a FA that is not present at 6' but appears at 10', whereas the arrowhead points to a FA that is present at 18' but has disappeared at 30'. The whole movie can be found in the online supplemental material (http://jcs.biologists.org/supplemental). Bar, 10 μm. (B) Quantitative analysis of the four FAs that were marked above (I-IV). The temporal changes of their average intensities and sizes are depicted. Often, neighboring FAs show different PY dynamics (compare FA I and II), and the changes in PY intensity are not always correlated in time with the growth of the FA. Note that the changes in PY level and FA size may be correlated in some cases (e.g. adhesions II and IV), or may be completely different (e.g. adhesions 1 and 3).

not significantly altered during the first 2-3 minutes after stimulation, and start to increase only 3-5 minutes after addition of the drug. Thus, the increase in tyrosine phosphorylation appears to be a consequence of nocodazole-induced protein recruitment rather than its cause. The notion that protein recruitment is the primary response to mechanical perturbation to integrin-mediated adhesions is in line with a recent report of Sawada and Sheetz (Sawada and Sheetz, 2002), who showed that the recruitment of FA molecules such as FAK and paxillin can be a direct consequence of tension-induced changes in the actin cytoskeleton and/or the integrin-associated adhesion plaque in membrane-permeabilized cell models.

Furthermore, the recruitment kinetics of different components after stimulation was not the same, leading to time-dependent changes in FA composition. As shown here, the initial increase in local intensities of all three proteins occurred essentially simultaneously, yet FAK levels reached a plateau at ~10 minutes after addition of nocodazole, whereas vinculin and paxillin levels usually reach maximal values at about 30 minutes. It is interesting to note that PY levels also reached a plateau at 10 minutes (Fig. 4), supporting the view that FAK is indeed a major regulator of tyrosine phosphorylation in FAs.

The immunofluorescence data discussed above provided strong, yet indirect, evidence for sequential molecular changes in FAs, induced by nocodazole, starting with the recruitment of FA plaque proteins and followed by tyrosine phosphorylation. To substantiate these findings directly at a single cell, or even single FA, level we had to develop an in vivo approach for visualizing tyrosine phosphorylation at a high spatial and temporal resolution. The YFP-dSH2 construct described here for the first time appears to serve as an accurate, quantitative PY reporter for live cells. This fusion protein readily localizes to FAs, its local intensities correlate linearly with those of anti-PY immunostaining and, at moderate expression levels, the protein has no apparent effect on the organization, PY levels and molecular composition of FAs.

As shown here, we have noticed that overexpression of YFP-dSH2 induces an increase in PY levels, most probably due to the protection of tyrosine-phosphorylated sites from phosphatases. Previous studies demonstrated that inhibition of PY phosphatases by chemical inhibitors can induce a rapid increase in the levels of FA-associated PY (Retta et al., 1996; Ayalon and Geiger, 1997). To avoid such effects, we have carefully defined a suitable range of expression levels of YFP-dSH2, which enables visualization of adhesion sites without altering their properties.

Another issue that should be considered here is the specificity of YFP-dSH2. Although SH2 domains, in general, may be selective for certain phosphorylated targets (Sawyer, 1998), the pp60Src-SH2 domain was found to bind to a broad spectrum of tyrosine-phosphorylated proteins, even when competing with other SH2 domains (Nollau and Mayer, 2001). Moreover, the distribution of YFP-dSH2 was essentially identical to that of several antibodies to PY, suggesting that the YFP-dSH2 molecule is a spatially and temporally faithful, and broad-specificity, reporter of local tyrosine phosphorylation in cell-matrix adhesions.

As discussed above, the YFP-dSH2 construct was designed and used primarily for directly timing the molecular events induced by nocodazole. For this purpose, we prepared two-color time-lapse movies in which YFP-dSH2- and CFP-vinculin-containing cells were exposed to the drug. Frame-by-frame analysis of the relative changes induced in YFP and CFP fluorescence revealed a strong early increase in vinculin levels, accompanied by FA growth, which takes place in almost every adhesion in the tested cells (Figs 7, 8). By contrast, the changes in local YFP-dSH2 levels during the same period were limited and non-uniform, confirming the notion that vinculin recruitment precedes the local increase in tyrosine phosphorylation by several minutes.

Another intriguing observation that emerged from the live-cell movies depicting the dynamics of tyrosine phosphorylation following nocodazole treatment is the lack of synchrony in the changes occurring in different adhesions of the same cell following stimulation. Thus, whereas in most adhesions the tyrosine-phosphorylated area was induced to grow following nocodazole treatment, the onset and rate of its expansion in individual adhesions were highly variable. This suggests that, even when the stimulation of FA assembly is 'global', changes in individual adhesions may be locally regulated or 'fine-tuned', owing to variations in local tension or other factors. These results also suggest that changes in local PY level and FA extension are not tightly linked and display complex, nonlinear relationships.

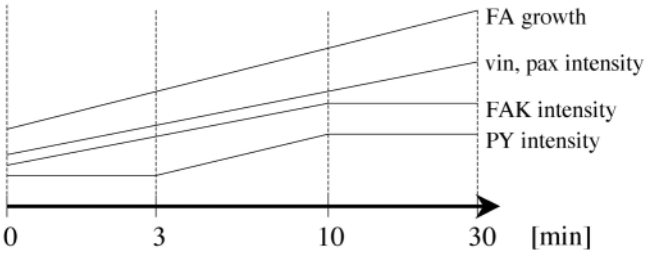

Fig. 10. A scheme summarizing the proposed sequence of dynamic molecular events during nocodazole-induced FA growth (see text for details). The time is shown on a logarithmic scale.

What is the sequence of molecular events leading to FA development following application of nocodazole? We propose (Fig. 10) that disruption of microtubules is accompanied by cellular contractility, which increases the mechanical tension at focal complexes or small FAs (Bershadsky, 1996). This mechanical stimulation activates, in turn, the recruitment of structural FA components, such as vinculin, paxillin and FAK, into focal complexes, leading to the growth of the adhesive structure. These responses are rather rapid, and are apparent within less than 2-3 minutes after addition of the drug. The accumulation of FAK and its pp60^{src}-induced activation result in an increase in local PY levels, which is typically delayed by 1-3 minutes after the protein recruitment. The increase in local tyrosine phosphorylation might, in turn, be involved in the downregulation of FA growth and the promotion of their turnover. This is in agreement with recent studies showing that FAs of pp60^{src}-null (Volberg et al., 2001) and FAK-null cells (L. H. Romer, T. Volberg and B.G., unpublished) fail to transform into fibrillar adhesions, and that excessive phosphorylation (e.g. by the deregulated pp60$^{v\text{-}src}$) leads to destruction of FAs (Kellie et al., 1986). Apparently, the first protein whose accumulation in growing FAs is arrested shortly after local phosphorylation increases is FAK itself, raising the possibility that its phosphorylation might downregulate its association with FAs. This notion is supported by recent studies (B. Z. Katz, L. H. Romer, S. Miyamoto, T. Volberg et al.., unpublished), showing that tyrosine phosphorylation of a C-terminal site on FAK interferes with its association with FAs.

The detailed molecular mechanisms involved in the nucleation and growth of FAs, as well as the precise role of tyrosine phosphorylation in FA development and maturation, are still poorly defined and remain to be elucidated in the future. Interestingly, several recent approaches might be instrumental in such studies. Among these are various fluorescent fusion proteins that can be expressed in cells, localize to FAs, and serve for dynamic analyses (Zamir et al., 2000; Laukaitis et al., 2001; Rottner et al., 2001). Particularly intriguing is the possibility of tracing tyrosine phosphorylation in live cells, using fluorescent derivatives of an SH2 domain, as described here. In addition, new approaches were recently developed for the direct measurement of mechanical forces in adhesion sites of live cells (Balaban et al., 2001; Riveline et al., 2001; Beningo et al., 2001). A combination of such approaches might provide us with deeper understanding of the molecular events underlying the formation and turnover of cell-matrix-adhesions, and shed new light on the role of tyrosine phosphorylation in these events.

We thank Eli Zamir for his help and valuable advice in setting up the computer programs used for image quantification. This study was supported by grants from the Minerva Foundation, Yad Abraham Center for Cancer Diagnosis and Therapy and the Israel Science Foundation. J.K. was supported by the Minerva foundation and by a Pacific Theatres Foundation Postdoctoral Fellowship. B.G. is the E. Neter Professor of Cell and Tumor Biology. A.D.B. holds the J. Moss Chair of Biomedical Research. Z.K. is the I. Pollack Professor of Biophysics.

References

Ayalon, O. and Geiger, B. (1997). Cyclic changes in the organization of cell adhesions and the associated cytoskeleton, induced by stimulation of tyrosine phosphorylation in bovine aortic endothelial cells. *J. Cell Sci*. **110**, 547-556.

Balaban, N. Q., Schwarz, U. S., Riveline, D., Goichberg, P., Tzur, G., Sabanay, I., Mahalu, D., Safran, S., Bershadsky, A., Addadi, L. and Geiger, B. (2001). Force and focal adhesion assembly: a close relationship studied using elastic micropatterned substrates. *Nat. Cell Biol*. **3**, 466-472.

Barry, S. T. and Critchley, D. R. (1994). The RhoA-dependent assembly of focal adhesions in Swiss 3T3 cells is associated with increased tyrosine phosphorylation and the recruitment of both pp125FAK and protein kinase C-delta to focal adhesions. *J. Cell Sci*. **107**, 2033-2045.

Beningo, K. A., Dembo, M., Kaverina, I., Small, J. V. and Wang, Y. L. (2001). Nascent focal adhesions are responsible for the generation of strong propulsive forces in migrating fibroblasts. *J. Cell Biol*. **153**, 881-888.

Bershadsky, A., Chausovsky, A., Becker, E., Lyubimova, A. and Geiger, B. (1996). Involvement of microtubules in the control of adhesion-dependent signal transduction. *Curr. Biol*. **6**, 1279-1289.

Bockholt, S. M. and Burridge, K. (1993). Cell spreading on extracellular matrix proteins induces tyrosine phosphorylation of tensin. *J. Biol. Chem*. **268**, 14565-14567.

Bradshaw, J. M., Mitaxov, V. and Waksman, G. (1999). Investigation of phosphotyrosine recognition by the SH2 domain of the Src kinase. *J. Mol. Biol*. **293**, 971-985.

Brown, M. T. and Cooper, J. A. (1996). Regulation, substrates and functions of src. *Biochim. Biophys. Acta*. **1287**, 121-149.

Calalb, M. B., Polte, T. R. and Hanks, S. K. (1995). Tyrosine phosphorylation of focal adhesion kinase at sites in the catalytic domain regulates kinase activity: a role for Src family kinases. *Mol. Cell. Biol*. **15**, 954-963.

Chrzanowska-Wodnicka, M. and Burridge, K. (1994). Tyrosine phosphorylation is involved in reorganization of the actin cytoskeleton in response to serum or LPA stimulation. *J. Cell Sci*. **107**, 3643-3654.

Chrzanowska-Wodnicka, M. and Burridge, K. (1996). Rho-stimulated contractility drives the formation of stress fibers and focal adhesions. *J. Cell Biol*. **133**, 1403-1415.

Clark, E. A., King, W. G., Brugge, J. S., Symons, M. and Hynes, R. O. (1998). Integrin-mediated signals regulated by members of the rho family of GTPases. *J. Cell Biol*. **142**, 573-586.

Enomoto, T. (1996). Microtubule disruption induces the formation of actin stress fibers and focal adhesions in cultured cells: possible involvement of the rho signal cascade. *Cell Struct. Funct.* **21**, 317-326.

Geiger, B. and Bershadsky, A. (2001). Assembly and mechanosensory function of focal contacts. *Curr. Opin. Cell Biol*. **13**, 584-592.

Geiger, B., Bershadsky, A., Pankov, R. and Yamada, K. M. (2001). Transmembrane extracellular matrix–cytoskeleton crosstalk. *Nat. Rev. Mol. Cell. Biol*. **2**, 793-805.

Geiger, B. and Bershadsky, A. (2002). Exploring the neighborhood. Adhesion-coupled cell mechanosensors. *Cell* **110**, 139-142.

Helfman, D. M., Levy, E. T., Berthier, C., Shtutman, M., Riveline, D., Grosheva, I., Lachish-Zalait, A., Elbaum, M. and Bershadsky, A. D. (1999). Caldesmon inhibits nonmuscle cell contractility and interferes with the formation of focal adhesions. *Mol. Biol. Cell* **10**, 3097-3112.

Kaverina, I., Krylyshkina, O. and Small, J. V. (1999). Microtubule targeting of substrate contacts promotes their relaxation and dissociation. *J. Cell Biol.* **146**, 1033-1043.

Kaverina, I., Krylyshkina, O., Beningo, K., Anderson, K., Wang, Y. L. and Small, J. V. (2002). Tensile stress stimulates microtubule outgrowth in living cells. *J. Cell Sci*. **115**, 2283-2291.

Kellie, S., Patel, B., Wigglesworth, N. M., Critchley, D. R. and Wyke, J. A. (1986). The use of Rous sarcoma virus transformation mutants with differing tyrosine kinase activities to study the relationships between vinculin phosphorylation, $pp60^{v\text{-}src}$ location and adhesion plaque integrity. *Exp. Cell Res.* **165**, 216-228.

Kimura, K., Ito, M., Amano, M., Chihara, K., Fukata, Y., Nakafuku, M., Yamamon, B., Feng, J., Nakano, T., Okawa, K. et al. (1996). Regulation of myosin phosphatase by Rho and Rho-associated kinase (Rho-kinase). *Science* **273**, 245-248.

Landt, O., Grunert, H. P. and Hahn, U. (1990). A general method for rapid site-directed mutagenesis using the polymerase chain reaction. *Gene* **96**, 125-128.

Laukaitis, C. M., Webb, D. J., Donais, K. and Horwitz, A. F. (2001). Differential dynamics of alpha 5 intregrin, paxillin, and alpha-actinin during formation and disassembly of adhesions in migrating cells. *J. Cell Biol*. **153**, 1427-1440.

Leopoldt, D., Lee, H. F. and Rozengurt, E. (2001). Calyculin A induces focal adhesion assembly and tyrosine phosphorylation of p125(Fak), p130(Cas), and paxillin in Swiss 3T3 cells. *J. Cell Physiol*. **188**, 106-119.

Liu, B. P., Chrzanowska-Wodnicka, M. and Burridge, K. (1998). Microtubule depolymerization induces stress fibers, focal adhesions, and DNA synthesis via the GTP-binding protein Rho. *Cell Adhes. Commun.* **5**, 249-255.

Martinez, R., Mathey-Prevot, B., Bernards, A. and Baltimore, D. (1987). Neuronal $pp60^{c\text{-}src}$ contains a six-amino acid insertion relative to its non-neuronal counterpart. *Science* **237**, 411-415.

Nobes, C. D. and Hall, A. (1995). Rho, rac, and cdc42 GTPases regulate the assembly of multimolecular focal complexes associated with actin stress fibers, lamellipodia, and filopodia. *Cell* **81**, 53-62.

Nollau, P. and Mayer, B. J. (2001). Profiling the global tyrosine phosphorylation state by Src homology 2 domain binding. *Proc. Natl. Acad. Sci. USA* **98**, 13531-13536.

Pankov, R., Cukierman, E., Katz, B.-Z., Matsumoto, K., Lin, D. C., Lin, S., Hahn, C. and Yamada, K. M. (2000). Integrin dynamics and matrix assembly; tensin-dependent translocation of alpha(5) beta (1) integrins promotes early fibronectin fibrillogenesis. *J. Cell Biol.* **148**, 1075-1090.

Pawson, T., Gish, G. D. and Nasha, P. (2001). SH2 domains, interaction modules and cellular wiring. *Trends Cell Biol.* **11**, 504-511.

Pletjushkina, O. J., Belkin, A. M., Ivanova, O. J., Oliver, T., Vasiliev, J. M. and Jacobson, K. (1998). Maturation of cell-substratum focal adhesions induced by depolymerization of microtubules is mediated by increased cortical tension. *Cell Adhes Commun.* **5**, 121-135.

Retta, S. F., Barry, S. T., Critchley, D. R., Defilippi, P., Silengo, L. and Tarone, G. (1996). Focal adhesion and stress fiber formation is regulated by tyrosine phosphatase activity. *Exp. Cell Res.* **229**, 307-317.

Ridley, A. J. and Hall, A. (1992). The small GTP-binding protein rho regulates the assembly of focal adhesions and actin stress fibers in response to growth factors. Cell **70**, 389-399.

Ridley, A. J. and Hall, A. (1994). Signal transduction pathways regulating Rho-mediated stress fibre formation: requirement for a tyrosine kinase. *EMBO J.* **13**, 2600-2610.

Ridley, A. J., Paterson, H. F., Johnston, C. L., Diekmann, D. and Hall, A. (1992). The small GTP-binding protein rac regulates growth factor-induced membrane ruffling. *Cell*. **70**, 401-410.

Riveline, D., Zamir, E., Balaban, N. Q., Schwarz, U. S., Ishizaki, T., Narumiya, S., Kam, Z., Geiger, B. and Bershadsky, A. D. (2001). Focal contacts as mechanosensors: externally applied local mechanical force induces growth of focal contacts by an mDia1-dependent and ROCK-independent mechanism. *J. Cell Biol*. **153**, 1175-1186.

Rottner, K., Hall, A. and Small, J. V. (1999). Interplay between Rac and Rho in the control of substrate contact dynamics. *Curr. Biol*. **9**, 640-648.

Rottner, K., Krause, M., Gimona, M., Small, J. V. and Wehland, J. (2001). Zyxin is not colocalized with vasodilator-stimulated phosphoprotein (VASP) at lammelipodial tips and exhibits different dynamics to vinculin, paxillin and VASP in focal adhesions. *Mol. Biol. Cell* **12**, 3103-3113.

Sambrook, J., Fritsch, E. F. and Maniatis, T. (1989). Molecular cloning: a laboratory manual. New York: Cold Spring Harbour Laboratory Press.

Sastry, S. K. and Burridge, K. (2000). Focal adhesions: a nexus for intracellular signaling and cytoskeletal dynamics. *Exp. Cell Res*. **261**, 25-36.

Sawada, Y. and Sheetz, M. P. (2002). Force transduction by Triton cytoskeletons. *J. Cell Biol.* **156**, 609-615.

Sawyer, T. K. (1998). Src homology-2 domains: structure, mechanisms, and drug discovery. *Biopolymers*. **47**, 243-261.

Schaller, M. D. (2001). Biochemical signals and biological responses elicited by the focal adhesion kinase. *Biochim. Biophys. Acta*. **1540**, 1-21.

Schneider, G. B., Gilmore, A. P., Lohse, D. L., Romer, L. H. and Burridge, K. (1998). Microinjection of protein tyrosine phosphatases into fibroblasts disrupts focal adhesions and stress fibers. *Cell Adhes. Commun.* **5**, 207-219.

Takaishi, K., Mino, A., Ikeda, W., Nakano, K. and Takai, Y. (2000). Mechanisms of activation and action of mDia1 in the formation of parallel stress fibers in MDCK cells. *Biochem. Biophys. Res. Commun.* **274**, 68-72.

Tominaga, T., Sahai, E., Chardin, P., McCormick, F., Courtneidge, S. A. and Alberts, A. S. (2000). GTPase and Src tyrosine kinase signaling. *Mol. Cell* **5**, 13-25.

Turner, C. E. (2000). Paxillin and focal adhesion signalling. *Nat. Cell Biol.* **2**, E231-E236.

Volberg, T., Geiger, B., Citi, S. and Bershadsky, A. D. (1994). Effect of protein kinase inhibitor H-7 on the contractility, integrity, and membrane anchorage of the microfilament system. *Cell. Motil. Cytoskeleton.* **29**, 321-338.

Volberg, T., Romer, L., Zamir, E. and Geiger, B. (2001). pp60(c-src) and related tyrosine kinases: a role in the assembly and reorganization of matrix adhesions. *J. Cell Sci*. **114**, 2279-2289.

Vuori, K. and Ruoslahti, E. (1995). Tyrosine phosphorylation of $p130^{Cas}$ and cortactin accompanies integrin-mediated cell adhesion to extracellular matrix. *J. Biol. Chem.* **270**, 22259-22262.

Watanabe, N., Kato, T., Fujita, A., Ishizaki, T. and Narumiya, S. (1999). Cooperation between mDia1 and ROCK in Rho-induced actin reorganization. *Nat. Cell Biol.* **1**, 136-143.

Zamir, E. and Geiger, B. (2001). Molecular complexity and dynamics of cell-matrix adhesions. *J. Cell Sci*. **114**, 3583-3590.

Zamir, E., Katz, B.-Z., Aota, S., Yamada, K. M., Geiger, B. and Kam, Z. (1999). Molecular diversity of cell-matrix adhesions. *J. Cell Sci*. **112**, 1655-1669.

Zamir, E., Katz, M., Posen, Y., Erez, N., Yamada, K. M., Katz, B. Z., Lin, S., Lin, D. C., Bershadsky, A., Kam, Z. and Geiger, B. (2000). Dynamics and segregation of cell-matrix adhesions in cultured fibroblasts. *Nat. Cell Biol.* **2**, 191-196.

Zhang, Q., Magnusson, M. K. and Mosher, D. F. (1997). Lysophosphatidic acid and microtubule-destabilizing agents stimulate fibronectin matrix assembly through Rho-dependent actin stress fiber formation and cell contraction. *Mol. Biol. Cell* **8**, 1415-1425.